American Journal of Pathology, Vol. 151, No. 2, August 1997

Loss of EDB$^+$ Fibronectin Isoform Is Associated with Differentiation of Alveolar Epithelial Cells in Human Fetal Lung

Hirokazu Arai,*† Hisanobu Hirano,‡ Sotaro Mushiake,§ Masahiro Nakayama,§ Goro Takada,† and Kiyotoshi Sekiguchi*

From the Departments of Pathobiology and Pathology,§ Osaka Medical Center and Research Institute for Maternal and Child Health, Izumi, Osaka, the Department of Pediatrics,† Akita University School of Medicine, Akita, and Otsuka Pharmaceutical Co., Ltd.,‡ Tokushima, Japan*

Cell-matrix interactions have been shown to regulate the development of the lung, particularly airway branching and alveolarization. Fibronectin is the major constituent of pulmonary extracellular matrix and exists in multiple isoforms arising from alternative RNA splicing. EDA and EDB are the two major alternatively spliced segments, the expression of which is regulated in a spatiotemporal and oncodevelopmental manner. In this study, we investigated immunohistochemically the distribution of the EDA- and EDB-containing fibronectin isoforms (referred to as EDA$^+$ fibronectin and EDB$^+$ fibronectin, respectively) in normal and hypoplastic human lungs at different gestational ages to explore the role of these fibronectin isoforms in alveolarization. EDA$^+$ fibronectin was expressed around the distal airspaces throughout the development of both normal and hypoplastic lungs. In contrast, the expression of EDB$^+$ fibronectin was restricted to the lung with morphologically immature acinar complex, typically observed in normally developing lungs of <30 gestational weeks or in hypoplastic lungs. To further confirm the restricted expression of EDB$^+$ fibronectin in immature acinar complex, we examined the correlation of EDB$^+$ fibronectin expression with that of the surfactant protein SP-A, a biochemical marker for the differentiated type II pneumocytes. A clear inverse relationship between the immunoreactivities for EDB$^+$ fibronectin and SP-A was observed in both control and hypoplastic lungs. Given the proposed importance of fibronectins in the differentiation of alveolar epithelial cells, our results suggest that the EDB segment plays a regulatory role in the differentiation of immature acinar epithelial cells into type II pneumocytes. The EDB segment may also serve as a new histochemical marker for the functional maturity of fetal lung tissues. *(Am J Pathol 1997, 151:403–412)*

The extracellular matrix (ECM) plays an important role in embryonic development and organogenesis. It serves as substrate for cell adhesion and migration and transduces biochemical signals that regulate proliferation, differentiation, and apoptosis of cells through interaction with integrins and other cell surface receptors.[1] In the lung, the interaction of pulmonary epithelial cells with their underlying ECM has been shown to regulate lung morphogenesis, particularly airway branching and alveolarization.[2,3] The alveolar basement membrane and its underlying mesenchyme contain various types of collagens, proteoglycans, and other glycoproteins such as laminin and fibronectin (FN).[2] *In vitro* studies have demonstrated that laminin and FN are essential regulators of pulmonary branching morphogenesis as well as epithelial differentiation into type II pneumocytes.[2–5]

FN is one of the major constituents of the pulmonary ECM and consists of two closely related subunit polypeptides with M_r of ~250,000. These subunits are encoded by a single FN gene and arise from a primary transcript by alternative RNA splicing at three distinct regions termed EDA, EDB, and IIICS.[1,6,7] The EDA and EDB segments are included or excluded from the mature mRNAs by exon skipping in a spatiotemporal and oncodevelopmental manner.[6,7] FNs containing these segments, often referred to as cellular-form FNs, are widely expressed in early embryonic tissues as well as in various types of tumors but are absent from most normal adult tissues.[6–10] Despite the characteristic patterns of expression of EDA$^+$ and EDB$^+$ FNs, the function of these alternatively spliced segments is only poorly understood.

The expression and distribution of FNs in the lung have been investigated at both protein and mRNA levels. FNs are present in the basement membrane of alveolar epithelium and capillary endothelium in both developing and adult lungs, although the immunostaining for FN is less intense in the adult lung than in the fetal lung.[11–14] Although the origin of the FNs deposited in the lung ECM is not well understood, biochemical analysis of the FNs insolubilized in the adult and fetal lung tissues has indicated that those in the adult lung are mostly of the plasma form, ie, FN lacking both EDA and EDB segments, whereas those in the fetal lung are essentially of the

Accepted for publication May 8, 1997.

Address reprint requests to Dr. Hirokazu Arai, Department of Pediatrics, Akita University School of Medicine, Hondo 1-1-1, Akita, Akita 010, Japan.

cellular form.[15] The detailed patterns of expression of the EDA^+ and EDB^+ FN isoforms during the morphogenetic process of human lung, however, remain to be determined.

In the present study, we investigated immunohistochemically the distribution of the EDA^+ and EDB^+ FNs in human developing lungs at different gestational ages to better understand the role of the FN isoforms in the alveolar formation and differentiation of alveolar epithelial cells. Special emphasis was given to the comparison of the staining patterns between normal and hypoplastic lungs, the latter of which was defined by low lung weight/body weight ratio and was associated with disorders including renal anomalies and chronic amniotic leakage. Although the pathogenesis of hypoplastic lung still remains to be defined, bronchiolar branching, acinar complexity, and acinar maturation are often retarded in the hypoplastic lungs,[16,17] suggesting that the abnormal expression of ECM components is associated with this anomaly. Our results show that FNs containing the EDB segment disappear from the lung ECM as immature acinar epithelial cells differentiate into type II pneumocytes, whereas those with the EDA segment are expressed throughout the development of the fetal lung. A significant delay in the disappearance of the EDB^+ FNs was observed in hypoplastic lungs along with the delay in the morphological maturation.

Materials and Methods

Lung Specimens

A total of 654 neonates who had died within 24 hours of birth or stillborn fetuses were autopsied at the Department of Pathology, Osaka Medical Center and Research Institute for Maternal and Child Health, from 1982 to 1994. Among them, 133 cases with freshly frozen lung tissues were selected in this study. The gestational age was estimated clinically by ultrasound echogram and confirmed by general appearance and organ maturation except lung. Cases with intrauterine infection or sepsis as well as macerated stillbirths and anencephaly were excluded. Cases whose postmorten examination was done longer than 24 hours after death were also excluded. Twenty-five of these cases were selected for control and hypoplastic lungs for this study.

Pulmonary hypoplasia was defined as a lung weight/body weight ratio under 0.012 (≧28 gestational weeks) or under 0.015 (<28 gestational weeks).[18] Seventeen cases were classified as pulmonary hypoplasia; the gestational ages ranged from 25 to 39 weeks. These cases had risk factors generally known to be associated with pulmonary hypoplasia, fifteen with renal anomalies and two with prolonged premature rupture of membrane. Eight cases whose lung weight/body weight ratio was within normal range were used as controls. Their gestational ages ranged from 21 to 39 weeks. The morphological staging of the lung was microscopically performed before beginning the study. All of the control cases were considered to be of appropriate histological appearances for their gestational ages and were not associated with marked pneumonia, hemorrhage, or edema. Tissue sections from the right upper lobe were used for immunohistochemical and *in situ* hybridization analyses throughout the present study.

Tissue Preparation

For immunohistochemical and *in situ* hybridization studies, fresh lung tissues were stored at −80°C until sectioning. Frozen tissues were cut into 5-μm sections using a cryostat and placed on poly-L-lysine-coated slides, which were air dried overnight and stored at −80°C until use.

For morphometric and morphological analysis, all lung tissue specimens were fixed with formalin, embedded in paraffin, and cut into 4-μm sections. These tissue sections were stained by hematoxylin and eosin (H&E).

Antibodies

Mouse monoclonal antibody specific to human EDB^+ FN, designated TFN01, was produced by immunizing mice with the recombinant protein A fusion protein containing the EDB segment and its flanking seventh and eighth type III modules of human FN and subsequent screening for positive reactivity with cellular FN purified from the conditioned medium of the SV40-transformed human fibroblast WI38VA13 and for negative reactivity with plasma FN.[19,20] The immunoglobulin isotype of TFN01 is IgM. The mouse IgG2a monoclonal antibody HHS01 was used as a specific probe for human EDA^+ FN as reported previously.[19,21] Rabbit antiserum raised against human plasma FN was used to detect all forms of FN (hereafter referred to as total FN). The mouse monoclonal antibody (PE10) against human surfactant apoprotein A (SP-A) was purchased from Dako Japan Co. (Kyoto, Japan).

Immunohistochemistry

The tissue sections were rehydrated in Tris-buffered saline (TBS) and then immersed in methanol containing 1.5% H_2O_2 for 20 minutes to block endogenous peroxidase. After three washes in TBS, the tissue sections were blocked with protein blocking agent (Immunon, Lipshaw, Pittsburgh, PA) for 30 minutes at room temperature in a humidified chamber. The tissue sections were then incubated overnight at 4°C with appropriately diluted primary antibodies: TFN01 (69 μg/ml), HHS01 (10.5 μg/ml), anti-human plasma FN antiserum (1:500), and PE10 (214 μg/ml). After three TBS washings, horseradish-peroxidase-labeled secondary antibodies, ie, anti-mouse IgM (Cappel, Organon Teknika Co., Durham, NC; 1:50 dilution) for TFN01, anti-mouse IgG (American Qualex, San Clemente, CA; 1:200 dilution) for HHS01 and PE10, or anti-rabbit IgG (Cappel; 1:100 dilution) for anti-human plasma FN antiserum, were applied for 60 minutes at room temperature in a humidified chamber. Slides were washed three times in TBS and incubated with diaminobenzidine tetrahydrochloride (Sigma Chemical Co., St. Louis, MO) for 15 minutes at room temperature. After

washing in distilled water, the tissue sections were counterstained with hematoxylin and then dehydrated and coverslipped.

The specificity of the immunohistochemistry was confirmed by negative reactivity upon 1) omitting the primary antibodies or 2) replacing the primary antibodies with diluted nonimmunized rabbit serum, mouse IgG, or mouse IgM (Zymed Laboratories, San Francisco, CA).

The immunohistochemical staining around the distal airspaces for EDB+ FN with TFN01 was graded as 0 (no staining detected), 1+ (staining beneath some but not all cells), 2+ (positive staining), and 3+ (intense staining). The grading of the SP-A expression was based on the staining positivity in the type II pneumocytes as follows: 0 (almost no positive cells in any distal airspace), 1+ (a few positive cells in some distal airspaces), 2+ (a few positive cells in all distal airspaces), 3+ (some positive cells in all distal airspaces). Five to ten tissue sections were made for each case, and blind assessments of these analyses were carried out for each case without any clinical or pathological information.

In Situ *Hybridization*

A 271-bp cDNA fragment encoding the 11th and 12th type I repeats was excised from the human FN cDNA pFH111 with *Eco*RI and *Acc*I and subcloned into pGEM4Z (Promega, Madison, WI). The plasmid was linearized by treatment with *Eco*RI (for the antisense probe) or *Hin*dIII (for the sense probe) at one or the other end of the polylinker site. The RNA probes were synthesized using either SP6 (sense) or T7 (antisense) RNA polymerase by adding digoxigenin-UTP (Boehring Mannheim, Mannheim, Germany). The RNA probes were recovered by ethanol precipitation and dissolved in diethylpyrocarbonate-treated, autoclaved double-distilled water.

Tissue sections were fixed in 4% paraformaldehyde for 20 minutes and then treated with proteinase K (Dako, Carpinteria, CA) at room temperature for 5 minutes. After washing, sections were sequentially treated with 0.2 N HCl for 10 minutes, followed by incubation with 100 mmol/L triethanolamine and 0.25% acetic anhydride. The slides were then washed in phosphate-buffered saline (PBS, pH 7.4), dehydrated, and air dried.

Each tissue section was covered with 50 μl of the hybridization solution (50% formamide, 10% dextran sulfate, 300 mmol/L NaCl, 20 mmol/L Tris/HCl (pH 8.0), 1X Denhardt's reagent, 0.02% sonicated salmon sperm DNA, 0.2% sarcosyl) containing 1 μg/ml RNA probe and incubated at 50°C in a humidified chamber for 16 hours. The sections were rinsed with 50% formamide in 2X sodium chloride/sodium citrate (SSC) at 50°C for 30 minutes and then treated with 1 μg/ml ribonuclease A in NTE (500 mmol/L NaCl, 10 mmol/L Tris/HCl (pH 7.5), 1 mmol/L EDTA) at 37°C for 30 minutes. The sections were washed in 0.1X SSC at 50°C three times, blocked with 1.5% Boehringer blocking reagent, and then incubated with anti-digoxigenin-antibody-alkaline-phosphatase conjugate (1:500 dilution; Boehringer Mannheim). After washing in 100 mmol/L Tris/HCl (pH 7.5) containing 150 mmol/L NaCl and immersion for 20 minutes in 100 mmol/L NaCl, 50 mmol/L $MgCl_2$, 100 mmol/L Tris/HCl (pH 9.5), the sections were incubated overnight with 338 μg/ml nitroblue tetrazolium and 175 μg/ml 5-bromo-4-chloro-3-indolyl-phosphate. The reaction was terminated by washing with 10 mmol/L Tris/HCl (pH 7.5) mmol/L EDTA. The slides were mounted using an aqueous mounting medium (Immunon, Lipshaw).

Morphometric and Morphological Analyses

The radial count, an index of acinar complexity, was measured in all cases by the method of Emery and Mithal.[22] Briefly, a line was drawn from the center of each respiratory bronchiole to the nearest connective tissue septum, and the number of distal airspaces cut by the line was counted. Ten to twenty counts from four to five tissue sections were made for each case.

Morphological staging of lung maturity was performed according to the criteria of Langston[17,23] and was classified into three categories: canalicular stage (development of acinus and its vascularization), saccular stage (subdivision of saccules), and alveolar stage (alveolar formation) based on the light microscopic appearance of the acinar complex. Blind assessments of these analyses were carried out for each case without any clinical or pathological information.

Statistical Analyses

Correlation coefficients were calculated with the Spearman's rank method. Probability values of $P < 0.05$ were accepted as significant.

Results

Morphometric and Morphological Analyses of Control and Hypoplastic Lungs

In this study, the lung weight/body weight ratio was used as the criterion for defining pulmonary hypoplasia. The lung weight/body weight ratio of all cases examined are summarized in Figure 1. In control cases, there was a significant decrease in the lung weight/body weight ratio that was dependent on the gestational age ($r = 0.916$; $P < 0.02$). In contrast, the ratio for all hypoplastic lung cases was under 0.012 irrespective of the gestational age.

Developmental maturity of the acinar complex in control and hypoplastic lungs was assessed morphometrically by means of the radial count. There was a clear positive correlation between the radial counts and the gestational age in control cases ($r = 0.886$; $P < 0.02$), although no positive correlation was observed in hypoplastic lung cases, the radial counts of which remained below 3.0 irrespective of gestational age (Figure 2). The morphological stages of the control and hypoplastic lungs, as determined by histological appearance, are summarized in Table 1. In control cases, the morpholog-

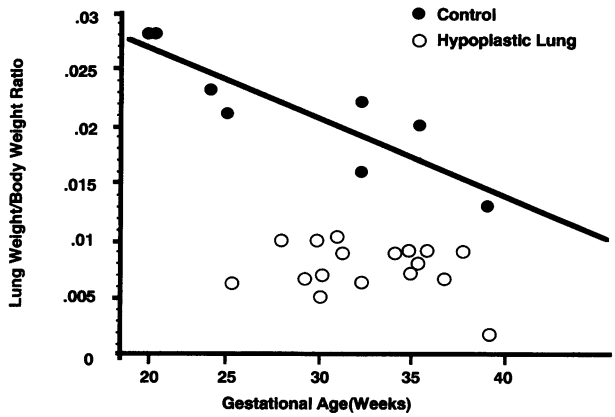

Figure 1. Lung weight/body weight ratio in control and hypoplastic lungs. The linear regression line for control lungs is presented.

ical stage was well correlated with the gestational age, although that of hypoplastic lung cases was significantly retarded when compared with the age-matched control cases. In particular, beyond 30 weeks of gestation, none of the control cases but more than 50% of hypoplastic lung cases were classified as canalicular stage. These results indicated that the developmental maturation of the lung was significantly retarded in many, if not all, cases with pulmonary hypoplasia as compared with the gestational-age-matched control cases.

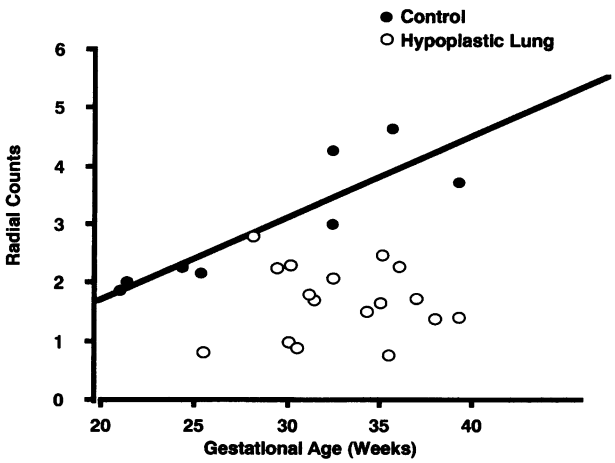

Figure 2. Radial counts in control and hypoplastic lungs. The regression line for control lungs is presented.

Immunohistochemical Analyses of EDA$^+$ and EDB$^+$ FNs

To examine how the expression of EDA+ and EDB+ FNs was regulated during the course of lung development, tissue specimens from the control cases of different gestational age were immunostained with monoclonal antibodies specific for EDA+ and EDB+ FNs (Figure 3).

At the canalicular stage, the mesenchymal tissues around the distal airspaces were still abundant (Figure 3, A and D). Both EDA+ and EDB+ FNs were detected in the basement membrane zone beneath the epithelial cells (Figure 3, B and E, C and F). Endothelial cells and smooth muscle cells surrounding blood vessels were also positive for EDA+ and EDB+ FNs (data not shown). Immunostaining for EDB+ FN was as intensive as that for EDA+ FN. Immunostaining for total FN was essentially identical to that for EDA+ FN (data not shown).

From the saccular to the alveolar stage, ie, beyond 30 gestational weeks, an increase in the gas-exchanging surface and thinning of mesenchymal tissues became evident (Figure 3, G and J). Immunostaining for EDA+ FN was almost ubiquitous (Figure 3, H and K). In septal tissues, the staining of the basement membrane zone beneath the epithelial cells could not be distinguished from the staining in the mesenchymal tissues. Staining for total FN was similar to that for EDA+ FN (data not shown). In contrast, EDB+ FN was barely detectable in septal tissues (Figure 3, I and L), although it remained detectable in endothelial cells of large vessels (data not shown).

In contrast to control tissue specimens, there was a considerable amount of mesenchymal tissues in most hypoplastic lungs (Figure 4, A and B). Distal airspaces were small and few in number, and the epithelial cells often consisted of cuboidal cells. EDA+ FN was strongly detected in the basement membrane zones beneath the epithelial cells (Figure 4, C and D). Total FN gave essentially the same immunostaining pattern as EDA+ FN (data not shown). EDB+ FN remained positively stained in the basement membrane zones beneath the epithelial lining even after 30 weeks of gestation (Figure 4, E and F). Staining for the EDB+ FN was, however, less intense than that for EDA+ FN.

These results indicated that, despite the continuous expression of EDA+ FN throughout the development of the lung, the expression of EDB+ FN was restricted to morphologically immature tissues, represented by those from normally developing lungs of <30 weeks of gestation or those from hypoplastic lungs. To correlate the

Table 1. Morphological Stage of Lung Specimens

Gestational age (weeks)	Control			Hypoplastic lung		
	Canalicular stage	Saccular stage	Alveolar stage	Canalicular stage	Saccular stage	Alveolar stage
20–24	3	0	0	0	0	0
25–29	1	0	0	1	2	0
30–34	0	2	0	5	2	0
35–39	0	1	1	3	4	0
Total	4	3	1	9	8	0

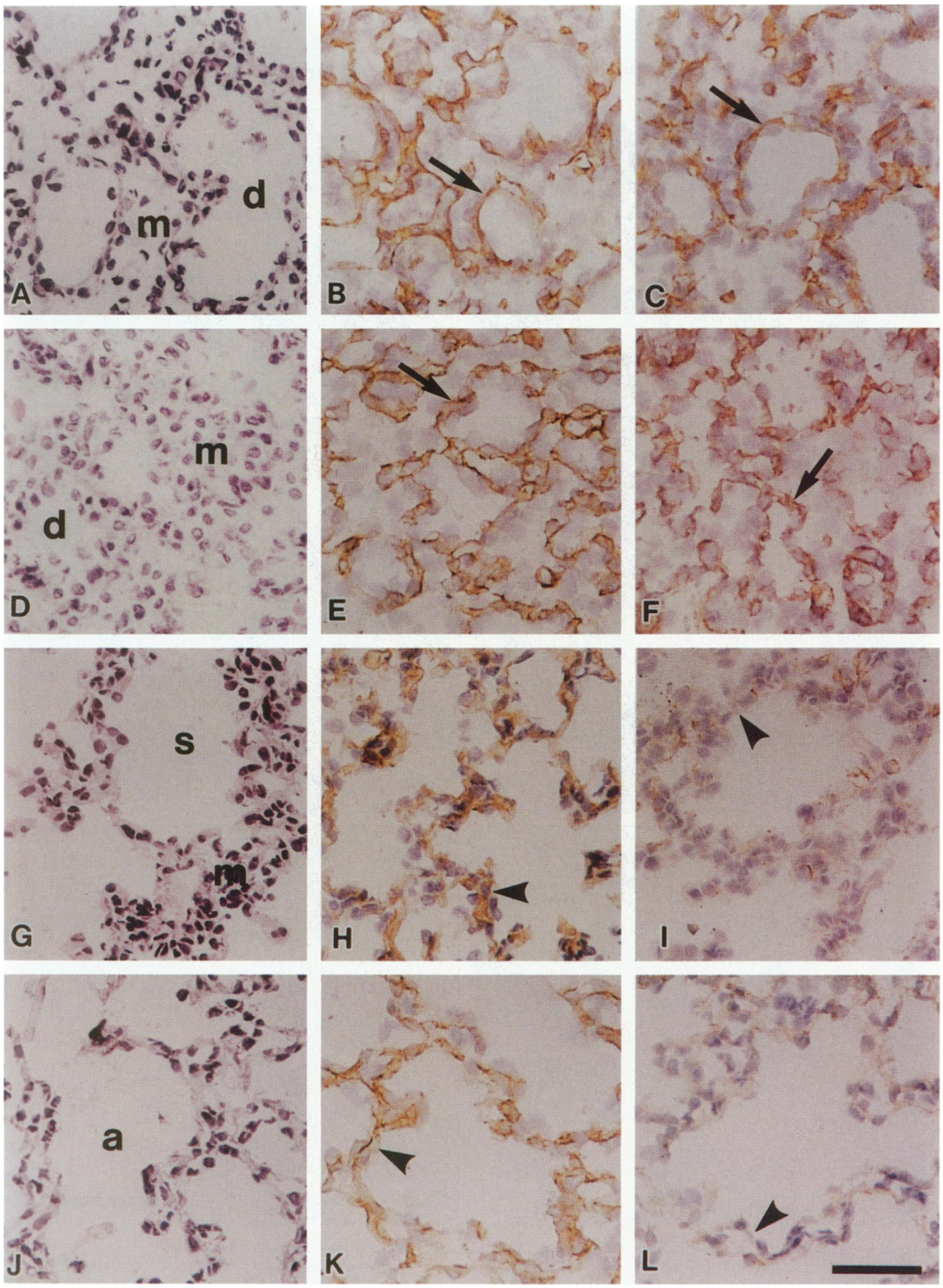

Figure 3. Immunohistochemical detection of EDA^+ and EDB^+ FNs at different morphological stages of normal developing lungs. Frozen tissue sections were stained by H&E (**A**, **D**, **G**, and **J**) or immunostained with anti-EDA (**B**, **E**, **H**, and **K**) or anti-EDB (**C**, **F**, **I**, and **L**) monoclonal antibodies. **A** to **C**: Canalicular-stage lung from a 21-week gestation fetus. Mesenchymal tissue (m) around the distal airspaces (d) was abundant. EDA^+ FN and EDB^+ FN were observed in the basement membrane zone (**arrow**) beneath the epithelial linings. **D** to **F**: Canalicular-stage lung from a 25-week gestation fetus. Staining patterns by H&E as well as with anti-EDA and anti-EDB antibodies were similar to those observed in **A** to **C**. **G** to **I**: Saccular-stage lung from a 32-week gestation fetus. Subdivision of saccules (s) and mesenchymal tissue (m) thinning were evident. Septal tissues (**arrowhead**) were positively stained with anti-EDA antibody but barely stained with anti-EDB antibody. **J** to **L**: Alveolar-stage lung from a 35-week gestation fetus. Thin-walled alveoli (a) were obvious. Staining patterns with anti-EDA and anti-EDB antibodies were similar to those observed in **H** and **I**. Bar, 50 μm.

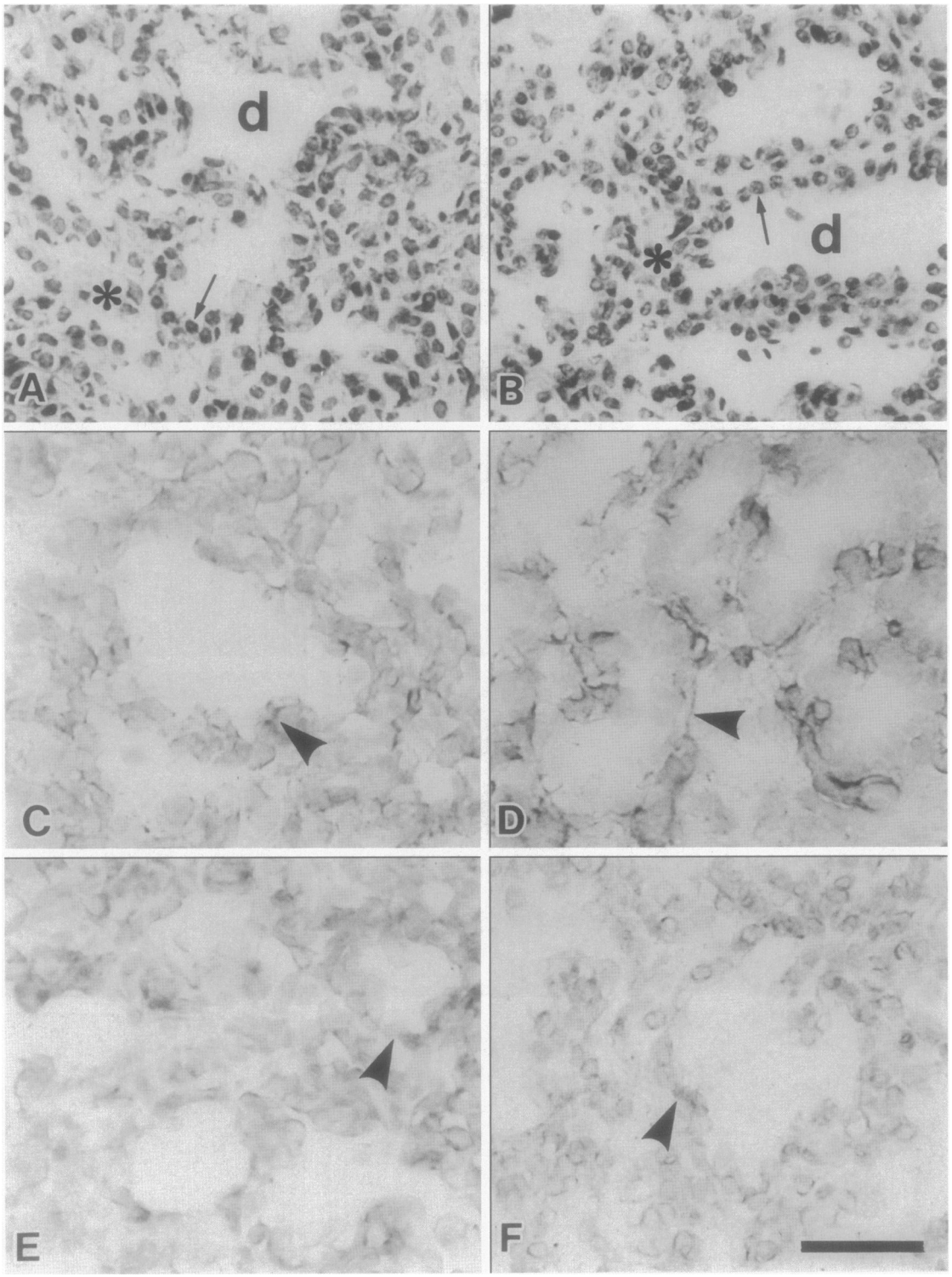

Figure 4. Immunohistochemical staining of hypoplastic lungs with anti-EDA and anti-EDB monoclonal antibodies. Frozen tissue sections were stained by H&E (**A** and **B**) or immunostained with anti-EDA (**C** and **D**) or anti-EDB (**E** and **F**) monoclonal antibodies. **A**, **C**, and **E**: Hypoplastic lung from a 31-week gestation fetus with dysplastic and hypoplastic kidney. There was a considerable amount of mesenchymal tissues (**asterisk**). Epithelial cells of distal airspaces (d) often consisted of cuboidal cells (**arrow**). EDA^+ FN staining was strongly detected in the basement membrane zone (**arrowhead**) beneath the epithelial lining. Staining for EDB^+ FN remained positive and showed the same pattern as for EDA^+ FN. **B**, **D**, and **F**: Hypoplastic lung from an infant of 37 weeks gestation with renal agenesis. Staining patterns by H&E as well as with anti-EDA and anti-EDB antibodies were similar to those observed in **A**, **C**, and **E**. Bar, 50 μm.

expression of EDB+ FN with developmental maturation of the lung, the staining intensities for EDB+ FN around distal airspaces were graded into four categories, ie, 0 to 3+, for both control and hypoplastic lungs (Table 2). Beyond 30 weeks of gestation, the tissues from most of the control cases gave 0 or only 1+ staining for EDB+

Table 2. Immunoreactivity around distal airspaces for anti-EDB+ fibronectin

Intensity of staining	20–24 weeks*	25–29 weeks	30–34 weeks	35–39 weeks
Control				
3+	2	1	0	0
2+	1	0	1	0
1+	0	0	0	1
0	0	0	1	1
Hypoplastic lung				
3+	0	1	2	0
2+	0	1	2	5
1+	0	0	3	1
0	0	1	0	1

3+, intense staining; 2+, positive staining; 1+, staining beneath some but not all cells; 0, no staining detected.
*Gestational age.

FN, although the tissues from 9 of the 14 hypoplastic lungs showed 2+ to 3+ reactivity, except one control case at 32 weeks of gestation that showed 2+ reactivity for EDB+ FN and one case with hypoplastic lung at 29 weeks of gestation that was negative for EDB+ FN expression.

Inverse Relationship between the Expression of EDB+ FN and SP-A

To further confirm the restricted expression of EDB+ FN in developmentally immature lung tissues, we examined the relationship of the levels of EDB+ FN expression with the levels of the expression of the surfactant protein SP-A, a biochemical marker for the differentiated type II pneumocytes.

Figure 5 shows the immunohistochemical detection of SP-A in lung tissues from two control cases of the same gestational age that differed in their reactivity with the antibody specific for EDB+ FN. SP-A was detected within the cytoplasm of alveolar epithelial cells, most likely type II pneumocytes, only in the tissue specimen negative for EDB+ FN (Figure 5, A and C). The tissue specimen positive for EDB+ FN was not immunostained with anti-SP-A antibody (Figure 5, B and D). A similar inverse relationship between the immunostaining for EDB+ FN and SP-A was also observed with the tissue specimens from two age-matched hypoplastic lungs (data not shown). To confirm the inverse relationship between the immunoreactivities for SP-A and EDB+ FN in lung tis-

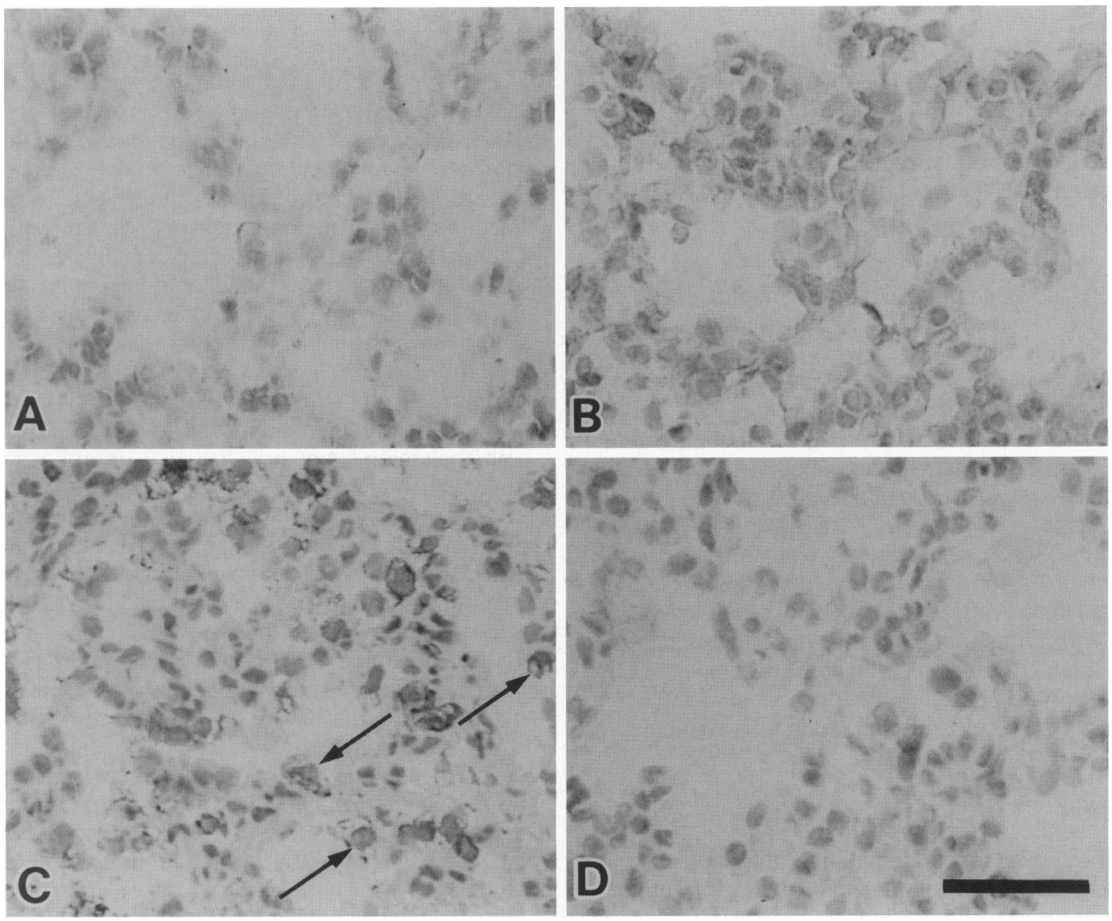

Figure 5. Inverse relationship in immunoreactivity with anti-EDB (**A** and **B**) and anti-SP-A (**C** and **D**) monoclonal antibodies in control lung tissues from two different fetuses (**A** and **C**; **B** and **D**) of 32 weeks gestation at saccular stage. The lung tissue negatively immunostained with anti-EDB antibody (**A**) was positively stained with anti-SP-A antibody in the cytoplasm of alveolar type II pneumocytes (**arrows, C**), whereas the tissue positively stained with anti-EDB antibody (**B**) was not reactive with anti-SP-A antibody (**D**). Bar, 50 μm.

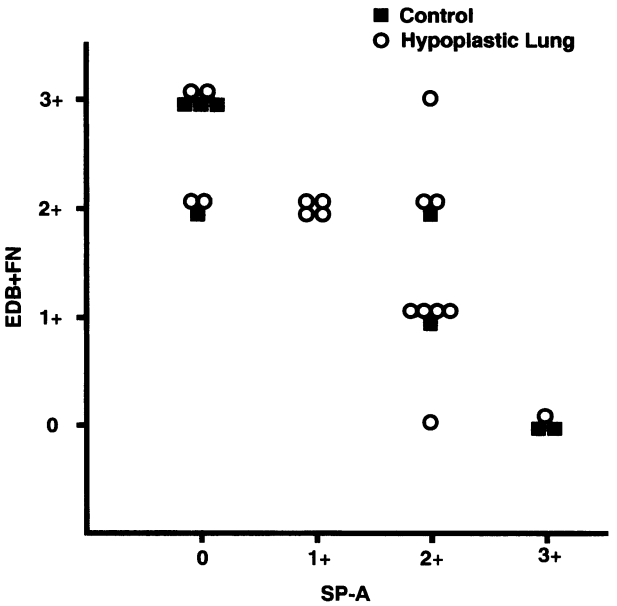

Figure 6. Relationship between the staining intensities for EDB$^+$ FN and SP-A in control and hypoplastic lungs. Immunostaining intensities with anti-EDB and anti-SP-A monoclonal antibodies were graded as described in Materials and Methods. There was a clear inverse relationship between the staining intensities with anti-EDB and anti-SP-A monoclonal antibodies for both control and hypoplastic lungs.

sues, the immunostaining intensities for SP-A, graded into four levels from 0 to 3+, was compared with those for EDB+ FN in all lung tissues examined in this study (Figure 6). A clear inverse correlation between the immunoreactivities for EDB+ FN and SP-A was observed in both control and hypoplastic lungs.

In Situ *Hybridization Analyses of FN mRNA Expression*

Although FNs were localized at the basement membrane zones beneath epithelial cells irrespective of the inclusion or exclusion of EDA and/or EDB segments, the immunohistochemistry could not discern whether the FNs were expressed by epithelial cells or underlining mesenchymal cells. To identify the cell types that synthesize and secrete FNs in developing lungs, we examined the cellular localization of FN transcripts by *in situ* hybridization using a digoxigenin-labeled cRNA probe that detects all FN isoforms. In both control (Figure 7, A and B) and hypoplastic (Figure 7C) lung specimens, the signals of FN transcripts were detected in the mesenchymal cells that surrounded distal airspaces but not in epithelial cells.

Discussion

Several lines of evidence indicate that the expression of EDA$^+$ and EDB$^+$ FNs is differentially regulated during the development of the lung. Using the nuclease protection analysis, Oyama et al[24] showed previously that EDB$^+$ FN is expressed only in the fetal but not in the adult lung, whereas EDA$^+$ FN is expressed in both fetal and adult lung tissues. Limited expression of EDB$^+$ FN in the fetal lung was also immunohistochemically demonstrated by Carnemolla et al[10] using the monoclonal antibody BC-1 that is specific for EDB$^+$ FN. Despite these previous studies, little has been known as to what stage of lung development the expression of EDB$^+$ FN is terminated and what roles EDA$^+$ and EDB$^+$ FNs play in the development of the lung. In the present study, we immunohistochemically examined the expression of the EDA$^+$ and EDB$^+$ FN isoforms in normal and hypoplastic human lungs at the different stages of development. Our results showed that, despite the continuous expression of EDA$^+$ FN throughout the lung development, the expression of EDB$^+$ FN beneath the epithelial lining of distal airspaces is restricted to the morphologically immature acinar complex, being observed with normally developing fetuses of less than 30 gestational weeks or with those with hypoplastic lungs. The loss of the EDB$^+$ FN expression appears to be associated with differentiation of alveolar epithelial cells, as the expression of EDB$^+$ FN is inversely related with the expression of SP-A in the distal airspaces, a well established biochemical marker of lung epithelial differentiation.[25–27] In support of the staining patterns of EDB$^+$ FN in this study, our preliminary results showed that immunohistochemical staining with another anti-EDB monoclonal antibody, BC-1, gave essentially the same results as obtained with TFN01 (H. Arai, unpublished observation).

Differentiation of lung immature acinar epithelial cells into type I and type II pneumocytes is crucial for neonates to survive, as the surfactant produced by type II pneumocytes is needed to counteract surface tension forces and to facilitate expansion of the alveoli, whereas the flattened type I pneumocytes provide efficient gas exchange surfaces.[2] The close association of the loss of EDB$^+$ FN with the differentiation of immature acinar epithelial cells into type II pneumocytes suggests that EDB$^+$ FN negatively regulates the differentiation of the alveolar epithelial cells. In support of this notion, EDB$^+$ FN was expressed in most of the hypoplastic lungs from fetuses of more than 30 gestational weeks, being in accordance with their significant retardation in morphological and functional maturation of distal airspaces. Although the specific role of EDB$^+$ FN isoforms in the differentiation of alveolar epithelial cells is unknown, involvement of FNs in the differentiation of alveolar epithelial cells has been demonstrated by *in vitro* studies using cultured alveolar epithelial cells.[2] Thus, the type II pneumocytes cultured on the substratum coated with FN alter their morphology from cuboidal to flattened shape with concomitant loss of cytoplasmic lamellar bodies, thus becoming more like type I pneumocytes.[2,28–30] Electron microscopic examination of neonatal rat lung tissues showed that FN was present in the basal and luminal surfaces of alveolar type I pneumocytes but not of type II pneumocytes.[31] Given the clear relationship between the loss of EDB$^+$ FN around the distal airspaces and the expression of SP-A in alveolar epithelial cells, EDB$^+$ FN may play a role in the differentiation of alveolar epithelial cells by interfering with the induction and/or maintenance of the differentiation phenotypes of type II pneumocyte.

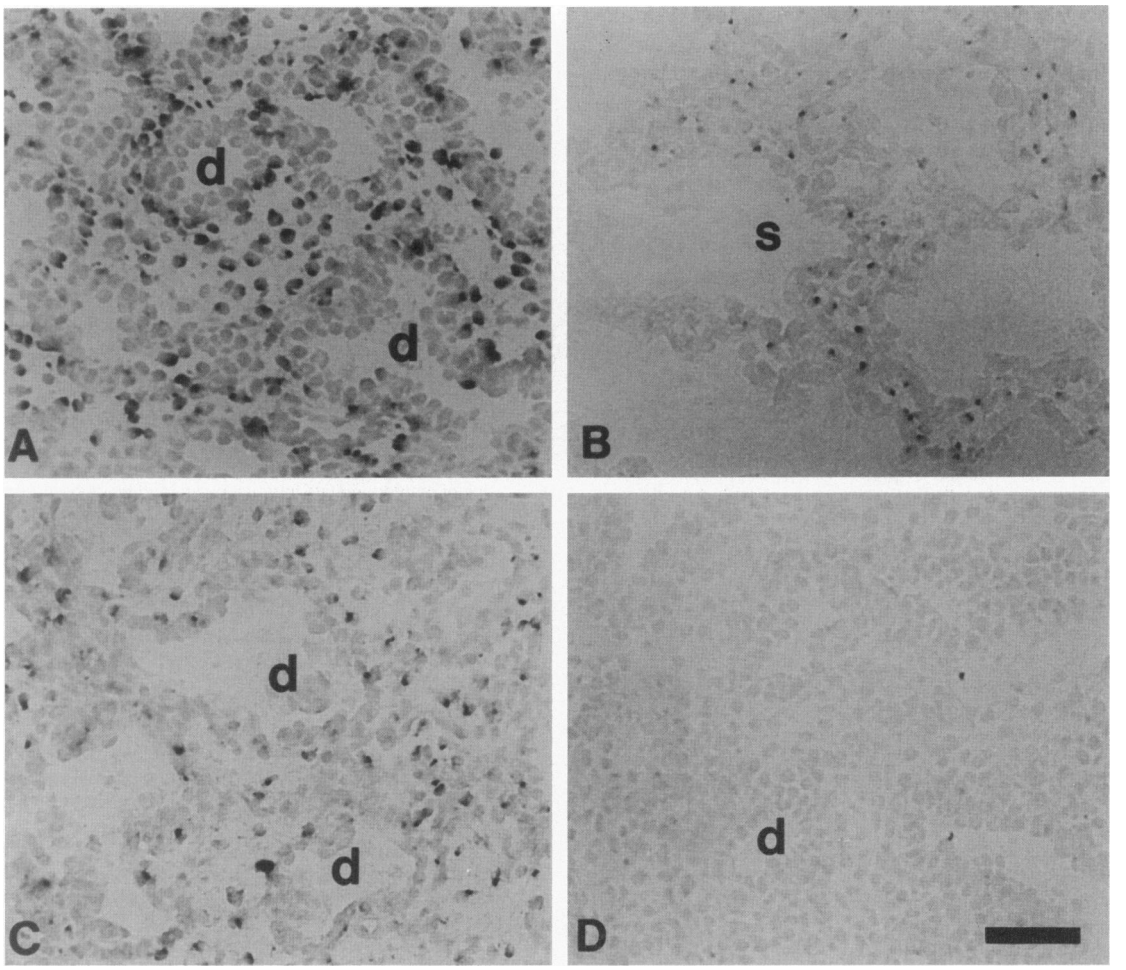

Figure 7. Localization of FN mRNA by *in situ* hybridization. Frozen sections of control (**A** and **B**) and hypoplastic (**C**) lungs were hybridized with an antisense cRNA probe recognizing all FN isoforms. In both cases, mesenchymal cells around distal airspaces (d) or saccules (s) express FN mRNA. More intense signals are detected with the lung at the canalicular stage from a 21-week gestation fetus (**A**) than with the lung at saccular stage from a 32-week gestation fetus (**B**). Hypoplastic lung from a 35-week gestation fetus with dysplastic and hypoplastic kidney (**C**) shows positive signals. In **D**, a sense cRNA probe was hybridized with a tissue specimen from the control lung of a 21-week gestation fetus. No significant signals are detected with the sense cRNA probe. Bar, 50 μm.

FNs are synthesized by many cell types including fibroblasts, endothelial cells, macrophages, and smooth muscle cells.[1] *In situ* hybridization using a FN cRNA probe showed that FN transcripts were expressed in the mesenchyme but not in the epithelial lining in both normally developing and hypoplastic lungs. These observations are consistent with the previous report by Sinkin et al[14] that FN mRNAs were detected in the mesenchyme and the vessel walls of rabbit developing lung but not in the alveolar epithelial cells irrespective of developmental stage. Although we did not identify the exact cell types expressing FN transcripts in the mesenchyme of the fetal lung, myofibroblasts could be one of the likely candidates. Myofibroblasts have been shown to express a high level of EDB+ FN.[32–34] The importance of myofibroblasts in alveolar formation has been demonstrated by Boström et al[35] with mice that are deficient in platelet-derived growth factor A chain expression. These mice failed to develop alveolar septa due to the loss of alveolar myofibroblasts.

The expression of EDB+ FN in tissues is primarily regulated at three distinct levels: transcription, RNA splicing, and protein degradation. The loss of the EDB+ FN around the distal airspaces in the saccular stage could be due to any one or a combination of them. Sinkin et al[14] reported that the levels of FN transcripts were the highest at the pseudoglandular stage and thereafter gradually decreased over the developmental period in rabbit. Our *in situ* hybridization studies also indicated that FN mRNA signals decreased over the developmental stages in normal developing lungs. Although no significant decreases in the immunostaining for EDA+ and total FNs were observed with human fetal lungs, we could not exclude the possibility that a decrease in the level of FN transcripts partly contributed to the loss of EDB+ FN around the distal airspaces. It appears to be more likely, however, that the loss of EDB+ FN is mainly due to an altered RNA splicing at the EDB exon. Clearly distinct patterns of alternative splicing at the EDB but not the EDA region were observed between fetal and adult lung tissues.[9,24] An increased degradation of the existing EDB+ FN may also be involved. EDB+ FN was shown to be more susceptible to proteolysis than other FN isoforms.[36] Consistent with this possibility is the observation that alveolar

type II pneumocytes produce proteinases that degrade FNs and other ECM components.[2]

In summary, the expression of EDB^+ FN was restricted to human developing lung tissues with a morphologically and functionally immature acinar complex. This loss of EDB^+ FN expression appears to be associated with the differentiation of immature acinar epithelial cells into type II pneumocytes. Although the role of EDB^+ FN in the development of the lung remains to be defined, these observations suggest that EDB^+ FN serves as a new histochemical marker for the functional maturity of fetal lung tissues.

Acknowledgments

We thank Dr. Akira Ishida, Dr. Hiroyuki Kitajima, and Dr. Masanori Fujimura for their support and helpful discussions.

References

1. Hynes RO: Fibronectins. New York, Springer-Verlag, 1990
2. Dunsmore SE, Rannels DE: Extracellular matrix biology in the lung. Am J Physiol 1996, 270:L3–L27
3. McGowan SE: Extracellular matrix and the regulation of lung development and repair. FASEB J 1992, 6:2895–2904
4. Schuger L, O'Shea S, Rheinheimer J, Varani J: Laminin in lung development: effects of anti-laminin antibody in murine lung morphogenesis. Dev Biol 1990, 137:26–32
5. Roman J, Crouch EC, McDonald JA: Reagents that inhibit fibronectin matrix assembly of cultured cells also inhibit lung branching morphogenesis in vitro: implications for lung development, injury, and repair. Chest 1991, 99:20S–21S
6. Ffrench-Constant C: Alternative splicing of fibronectin: many different proteins but few different functions. Exp Cell Res 1995, 221:261–271
7. Kornblihtt AR, Pesce CG, Alonso CR, Cramer P, Srebrow A, Werbajh S, Muro AF: The fibronectin gene as a model for splicing and transcription studies. FASEB J 1996, 10:248–257
8. Ffrench-Constant C, Hynes RO: Alternative splicing of fibronectin is temporally and spatially regulated in the chicken embryo. Development 1989, 106:375–388
9. Pagani F, Zagato L, Vergani C, Casari G, Sidoli A, Baralle FE: Tissue-specific splicing pattern of fibronectin messenger RNA precursor during development and aging in rat. J Cell Biol 1991, 113:1223–1229
10. Carnemolla B, Balza E, Siri A, Zardi L, Nicotra MR, Bigotti A, Natali PG: A tumor-associated fibronectin isoform generated by alternative splicing of messenger RNA precursors. J Cell Biol 1989, 108:1139–1148
11. Roman J, McDonald JA: Expression of fibronectin, the integrin $\alpha 5$, and α-smooth muscle actin in heart and lung development. Am J Respir Cell Mol Biol 1992, 6:472–480
12. Chen WT, Chen JM, Mueller SC: Coupled expression and colocalization of 140K cell adhesion molecules, fibronectin, and laminin during morphogenesis and cytodifferentiation of chick lung cells. J Cell Biol 1986, 103:1073–1090
13. Snyder JM, O'Brien JA, Rodgers HF: Localization and accumulation of fibronectin in rabbit fetal lung tissue. Differentiation 1987, 34:32–39
14. Sinkin RA, Sanders RS, Horowitz S, Finkelstein JN, Lomonaco MB: Cell-specific expression of fibronectin in adult and developing rabbit lung. Pediatr Res 1995, 37:189–195
15. Sekiguchi K, Klos AM, Hirohashi S, Hakomori S: Human tissue fibronectin: expression of different isotypes in the adult and fetal tissues. Biochem Biophys Res Commun 1986, 141:1012–1017
16. Nakamura Y, Harada K, Yamamoto I, Uemura Y, Okamoto K, Fukuda S, Hashimoto T: Human pulmonary hypoplasia: statistical, morphological, morphometric, and biochemical study. Arch Pathol Lab Med 1992, 116:635–642
17. Thurlbeck WM: Prematurity and the developing lung. Clin Perinatol 1992, 19:497–519
18. Askenazi SS, Perlman M: Pulmonary hypoplasia: lung weight and radial alveolar count as criteria of diagnosis. Arch Dis Child 1979, 54:614–618
19. Hirano H, Tachikawa T, Hino K, Sakashita E, Sekiguchi K: Development of enzyme-linked immunosorbent assay (ELISA) for the detection of cellular type fibronectin by EDA-region specific monoclonal antibody (in Japanese). J Clin Lab Instrum Reagents 1992, 15:179–184
20. Hirano H, Tachikawa T, Oyama F, Titani K, Sekiguchi K: Coordinated regulation of alternative splicing of fibronectin pre-mRNA at ED-A and ED-B regions. Mol Biol Cell 1992, 3(suppl):223a
21. Hino K, Shiozawa S, Kuroki Y, Ishikawa H, Shiozawa K, Sekiguchi K, Hirano H, Sakashita E, Miyashita K, Chihara K: EDA-containing fibronectin is synthesized from rheumatoid synovial fibroblast-like cells. Arthritis Rheum 1995, 38:678–683
22. Emery JL, Mithal A: The number of alveoli in the terminal respiratory unit of man during late intrauterine life and childhood. Arch Dis Child 1960, 35:544–547
23. Langston C, Kida K, Reed M, Thurlbeck WM: Human lung growth in late gestation and in the neonate. Am Rev Respir Dis 1984, 129:607–613
24. Oyama F, Hirohashi S, Shimosato Y, Titani K, Sekiguchi K: Oncodevelopmental regulation of the alternative splicing of fibronectin premessenger RNA in human lung tissues. Cancer Res 1990, 50:1075–1078
25. Rooney SA, Young SL, Mendelson CR: Molecular and cellular processing of lung surfactant. FASEB J 1994, 8:957–967
26. Kuroki Y, Dempo K, Akino T: Immunohistochemical study of human pulmonary surfactant apoproteins with monoclonal antibodies: pathologic application for hyaline membrane disease. Am J Pathol 1986, 124:25–33
27. Hallman M, Arjomaa P, Mizumoto M, Akino T: Surfactant proteins in the diagnosis of fetal lung maturity. I. Predictive accuracy of the 35 kD protein, the lecithin/sphingomyelin ratio, and phosphatidylglycerol. Am J Obstet Gynecol 1988, 158:531–535
28. Casale JM, Rochat TR, Moore KC, Hunninghake GW: Stereologic analysis of rat type II alveolar cells in vitro. J Lab Clin Med 1987, 110:767–772
29. Rannels SR, Fisher CS, Heuser LJ, Rannels DE: Culture of type II pneumocytes on a type II cell-derived fibronectin-rich matrix. Am J Physiol 1987, 253:C759–C765
30. Rannels SR, Rannels DE: The type II pneumocyte as a model of lung cell interaction with the extracellular matrix. J Mol Cell Cardiol 1989, 21:151–159
31. Rosenkrans WA, Albright JT, Hausman RE, Penney DP: Ultrastructural immunocytochemical localization of fibronectin in the developing rat lung. Cell Tissue Res 1983, 234:165–177
32. Brouty-Boyé D, Magnien V: Myofibroblast and concurrent ED-B fibronectin phenotype in human stromal cells cultured from non-malignant breast tissue. Eur J Cancer 1994, 30A:66–73
33. Brouty-Boyé D, Raux H, Azzarone B, Tamboise A, Tamboise E, Béranger S, Magnien V, Pihan I, Zardi L, Israël L: Fetal myofibroblast-like cells isolated from post-radiation fibrosis in human breast cancer. Int J Cancer 1991, 47:697–702
34. Pujuguet P, Hammann A, Moutet M, Samuel JL, Martin F, Martin M: Expression of fibronectin $ED\text{-}A^+$ and $ED\text{-}B^+$ isoforms by human and experimental colorectal cancer: contribution of cancer cells and tumor-associated myofibroblasts. Am J Pathol 1996, 148:579–592
35. Boström H, Willetts K, Pekny M, Levéen P, Lindahl P, Hedstrand H, Pekna M, Hellström M, Gebre-Medhin S, Schalling M, Nilsson M, Kurland S, Törnell J, Heath JK, Betsholtz C: PDGF-A signaling is a critical event in lung alveolar myofibroblast development and alveogenesis. Cell 1996, 85:863–873
36. Zardi L, Carnemolla B, Siri A, Petersen TE, Paolella G, Sebastio G, Baralle FE: Transformed human cells produce a new fibronectin isoform by preferential alternative splicing of a previously unobserved exon. EMBO J 1987, 6:2337–2342